Restricted entry of globular cluster stars to the asymptotic giant branch

Simon W. Campbell[1], Valentina D'Orazi[2,1], David Yong[3], Thomas N. Constantino[1], John C. Lattanzio[1], Richard J. Stancliffe[3,4], George C. Angelou[1], Elizabeth C. Wylie-de Boer[3], Frank Grundahl[5]

[1]*Monash Centre for Astrophysics, School of Mathematical Sciences, Monash University, Melbourne, VIC 3800, Australia.*

[2]*Department of Physics & Astronomy, Macquarie University, Balaclava Rd, North Ryde, Sydney, NSW 2109, Australia.*

[3]*Research School of Astronomy and Astrophysics, Australian National University, Weston, ACT 2611, Australia*

[4]*Argelander-Insitut für Astronomie, Universität Bonn, Auf dem Hügel 71, 53121 Bonn, Germany.*

[5]*Stellar Astrophysics Centre, Department of Physics and Astronomy, Aarhus University, Ny Munkegade 120, DK-8000 Aarhus C, Denmark.*

Summary Paragraph

The vast majority of stars in the Universe are not massive enough to end their lives as supernovae. Low-mass stars, including the Sun, instead experience a final, non-explosive nuclear burning stage – the Asymptotic Giant Branch (AGB) phase. Containing millions of low-mass stars Milky Way globular clusters are used as testbeds to constrain stellar evolution theory. Here we show, by using sodium as a spectroscopic 'chemical tracer' in stars, a striking discovery: many stars in globular clusters actually die out before reaching their AGB phase. This finding has a number of ramifications, including (i) cluster star counts used to test stellar evolution timescales and deduce cluster helium abundances are not reliable if they involve AGB stars, (ii) new input physics is required for stellar evolution codes to model this phenomenon, and (iii) there may be a 'loss' of integrated light from extragalactic clusters due to lower numbers of these bright stars.

Introduction

Stellar evolution theory[1–3], underpins much of modern astronomy and astrophysics. Apart from their output of electromagnetic radiation in virtually all parts of the spectrum, stars also drive the chemical evolution of the Universe through their internal nucleosynthesis and subsequent ejection of processed gas and dust via supernovae explosions and stellar winds. In the study of distant galaxies it is the stars, although unresolved individually, which, through their light, provide the wealth of kinematic and chemical information which we use to investigate the greater Universe.

The vast majority of stars do not end their lives as supernovae because they are not massive enough ($\lesssim 10$ $M_\odot$). Standard stellar evolution theory predicts that a low-mass star, such as the Sun, experiences four key nuclear burning phases: the main sequence (MS, core H burning), the red giant branch (RGB, H-shell burning), the horizontal branch (HB, core helium burning) and finally the asymptotic giant branch (AGB, H-shell and He-shell burning). During the AGB phase the star loses copious amounts of mass from its surface via stellar winds, thereby contributing to the chemical evolution of the Universe. The star finally ends its evolution as a naked core composed primarily of carbon and oxygen – a white dwarf (WD).

While most phases of evolution have been well studied both photometrically and spectroscopically[4–6], the AGB phase has received less attention. This is because the AGB is difficult to study observationally, for two main reasons. First, there are relatively few AGB stars, a consequence of their short lifetimes, and secondly it is difficult to identify them in colour-magnitude diagrams (CMDs, constructed by plotting the colours of stars against their brightnesses) because they lie in similar colour-magnitude space as RGB stars. Thus, in order to study a large homogeneous sample of AGB stars, a very large homogeneous stellar population is needed so that the number of AGB stars is substantial. High-quality photometry is also needed, to differentiate the two giant branches in CMDs. Galactic globular clusters (GCs) are one of the few objects in which these two constraints can be met. Their stellar populations are large ($10^4 \rightarrow 10^6$ stars) and they are close enough for modern telescopes to resolve individual stars and collect high-quality photometric data. High-resolution spectroscopic observations are also feasible, providing a plethora of information on chemical abundances and kinematics. For these reasons, and since the CMDs of

GCs show a convenient 'snapshot' of all phases of evolution, GCs are well known for being very useful 'laboratories' for testing and constraining low-mass stellar evolution theory in general[7–9].

Recent high quality photometry[10,11] has allowed our group to identify large samples of AGB stars in a variety of GCs. Using this sample we are pursuing a broad investigation into AGB stars with medium-resolution spectral observations in 9 GCs[12,13]. Preliminary results from that study have motivated us to pursue the higher resolution spectroscopic study presented here.

Although still amongst the most homogeneous stellar populations known, it is now well established that GCs are not the simple, single stellar populations they were once thought to be. All well-studied GCs are known to contain (at least) two populations with different light element (e.g. C, N, Na) contents. Early spectroscopic work showed this through observations of molecular band absorption[14]. For example the star-to-star distribution of cyanogen (CN, used as a proxy for N) band strengths in a GC is usually bimodal, with one population of stars having strong CN absorption and the other weak (CN-strong vs CN-weak stars). From high resolution spectroscopy it is now clear that every GC contains at least two populations/generations of stars[6,15] – a first generation (FG), having higher abundances of C and O but lower abundances of He, N and Na, and a second generation (SG), having enhanced N and Na but lower C and O. The SG stars are thought to have formed from the ejected gas of the short-lived intermediate-mass ($\sim 4 \rightarrow 9$ M$_\odot$) stars of the FG population[15], since the abundance variations (anti)correlate in a way that is highly suggestive of nuclear processing through the CNO cycles (and sometimes also the Ne-Na, Mg-Al chains). There is some evidence that the SG stars also have enhanced He[16,17], which ties in with the CNO cycling since He is the main product of H burning (He is very difficult to measure directly in stars). The proportions of these populations are usually around 40:60 (FG:SG).

Early work on AGB stars in GCs hinted at possible chemical abundance differences between the AGB and other phases of evolution. In particular, a study of NGC 6752 reported that their entire sample of 12 AGB stars appeared to be CN-weak[14]. This was in contrast to their RGB sample which showed a bimodal mix of CN-weak and CN-strong stars, roughly in a ratio of 40:60. This difference is quite unexpected since a surface abundance change going from the RGB to AGB is not predicted by standard stellar evolution. The same authors speculated that this difference could also come about if the CN-strong stars were failing to reach the AGB phase for some reason. Other studies found different results for different GCs, for example the AGB population of M5 appeared to be dominated by CN-strong stars[18]. These possible AGB-RGB differences are interesting considering that all other phases of evolution show roughly the same proportions of CN-weak to CN-strong stars within each GC. The early results were however based on small samples of stars. CN molecular band strengths are also known to be affected by a complex interplay between the relative abundances of C, N, O, especially at the temperatures typical of cool giant stars[19,20]. Furthermore, it is well established that low-mass stars alter their surface abundances of C and N in situ along the RGB via ‘deep-mixing’[21,22]. For these reasons there has been uncertainty in the reality of there being a difference in abundance distributions between the AGB and other phases of evolution. A more concrete determination of abundance variations is the measurement of elemental sodium, since it is not affected by molecular band formation uncertainties and stars of this mass can not alter their Na abundances in situ. Here we report on our survey of Na abundances of NGC

6752 giant stars. NGC 6752 is ideal for this study because it is well-studied, nearby, massive and suffers little interstellar reddening.

Stellar Sample and Results

Our stellar sample includes 20 AGB stars and 24 RGB stars. Figure 1 shows the sample against the greater CMD dataset[10]. We include RGB stars as a control group, since it has previously been shown that this evolutionary population harbours the standard abundance distributions, including the well-known Na-O anticorrelation present in all GCs[23]. RGB stars also have similar surface temperatures and gravity to AGB stars, making comparisons more direct.

In Figure 2 we show the sodium abundance results for both the AGB and RGB samples. The RGB sample shows the usual spread in [Na/Fe][1] of roughly 1 dex. On the other hand the AGB result is very striking – every single one of the AGB stars in our sample lies at the low end of the RGB distribution. The upper envelope of the AGB sodium abundances is located at about [Na/Fe] $= 0.18$ dex (dotted line in Fig. 2). Interestingly this corresponds very closely to a previous RGB study[6] that defines the FG population as having [Na/Fe] $\lesssim 0.2$ (their 'Primordial' population). Using either value as the border for the definition of Na-poor and Na-rich stars we find the proportions of Na-poor to Na-rich RGB stars in our data to be 30:70. Again this corresponds well to the roughly 30:70 proportions found previously[6][2]. Thus, surprisingly, *all* of our AGB stars appear to be FG stars.

---

[1] This notation shows the abundance ratios of two elements in a star's atmosphere relative to the solar ratio: [X/Y] $= \log_{10}(N_X/N_Y)_{star} - \log_{10}(N_X/N_Y)_{Sun}$, where the N_i are the number of atoms of each elemental species.

[2] The previous study also reports a third population but only at the level of about 2%.

The range in [Na/Fe] in our AGB sample very small, with a mean of -0.07 and a standard deviation of 0.10 dex. This scatter is comparable to our internal uncertainties (Table 1), indicating that the AGB stars may have a uniform abundance of Na. Assuming the 30:70 Na-poor:Na-rich distribution as seen on the RGB, the probability of randomly selecting 20 Na-poor AGBs is extremely low, especially considering that we have derived Na abundances for almost all of the AGB stars in the region covered by the photometric dataset (Fig.). It now appears certain that the entire population of SG stars, having elevated levels of Na and N (along with low levels of C and O), do not make it to the AGB phase. This is a huge effect since the SG contains the majority of the stars in NGC 6752. Furthermore, there is the possibility that some Na-poor stars may also fail to reach the AGB. This indicates that *at least* 70% of the stars do not ascend the AGB.

Discussion

Although the theory that some stars may not ascend the AGB has previously been discussed in the literature from both theoretical and observational perspectives[14,24], the result presented here is the first conclusive confirmation of the phenomenon. Moreover, we can readily identify which stars do not ascend the AGB based on their Na content ([Na/Fe] $\gtrsim 0.18$ dex).

An obvious consequence of such a large proportion of stars avoiding the AGB is that there should currently be many fewer stars in the AGB phase than expected. A detailed study reporting star counts of GC populations finds a value of $R_2 = N_{AGB}/N_{HB} \sim 0.06$ for NGC 6752[11]. This is one of the lowest R_2 values in their GC sample. The GCs with the two highest R_2 values in their sample (M 5 and M 55) could be assumed to provide an upper limit to R_2 since R_2 is fairly insensitive to metallicity, He abundance, and GC age[25]. Interestingly this upper value is ~ 0.18 – a factor of 3 higher than that of NGC 6752. This is indeed consistent with our result of $\gtrsim 70\%$ of stars not ascending the AGB. Current model predictions for R_2 tend to be lower than 0.18, being around $0.12 \rightarrow 0.15$[25,26], however the models are known to suffer from significant uncertainties[26]. We note that the observed R_2 value for NGC 6752 is still at least a factor of 2 smaller than the model predictions.

It has long been speculated that the composition differences between the FG and SG populations could have an effect on the CMD structure of GCs[14]. Recent work has revealed that this does appear to be true. A new study on M4, which has both a red HB (RHB) and a blue HB (BHB), has shown that all RHB stars in their sample are Na-poor, whilst all their BHB stars are Na-rich[27]. They infer that the He content must be different between the two Na populations since it is not expected that Na (or N) could affect the position of stars in the HB, while He can[7,16,28]. In the case of NGC 6752 a sample of HB stars from the redder end of the HB (NGC 6752 only has a BHB) was shown to exclusively[3] contain Na-poor stars[29]. The same stars have a uniform He abundance that is consistent with Big Bang theory predictions (Y $= 0.245$), as expected for a FG population. Thus it appears that the bluer (presumably Na-rich) HB stars must avoid AGB ascent – leaving only the redder, Na-poor HB stars to populate the AGB of NGC 6752. Combining this information with our estimate of the proportion of stars that do not ascend the AGB, we can estimate what HB colour delineates the border between the two groups. Since our $uvby$ CMD dataset is not complete at the

---

[3] That study also reports one star with elevated Na abundance, but, as noted by the authors, the star has evolved off the HB and probably started from a much bluer position.

bluest end of the HB, we obtained a very high quality UBV photometric dataset[30] for this purpose. We counted HB stars in the $U, U - V$ plane, starting at the red edge of the HB at $U - V = 0.25$. The total number of HB stars was found to be 320. Thus we expect the reddest 96 stars (30%) to eventually ascend the AGB. We find that this number of redder HB stars corresponds to an 'ascension cut-off' in $U - V$ of -0.30. Interestingly this is exactly the colour for the Grundahl jump[10,30]. The Grundahl jump is a well-known discontinuity in the HB morphology seen in $uvby$ and UVB photometry. It is seen in all GCs studied to date whose HB extends beyond $\mathrm{T}_{eff} \gtrsim 11,500$ K. Explanations of this discontinuity include radiative levitation of elements heavier than carbon and nitrogen in the high-temperature atmospheres of these stars[10], or the combination of post-zero-age HB evolution and diffusion effects[30]. At face value, it appears that all stars bluer than the Grundahl jump do not ascend the AGB, at least in NGC 6752. This may represent further evidence that there is some fundamental change in the stellar atmosphere structure and/or mass-loss physics occurring at the Grundahl jump temperature[10,31]. We note that it is these extremely blue HB stars that are considered to be the source of excess UV flux in the spectra of elliptical galaxies[32].

Theoretical models show that a star on the HB will not ascend the AGB if it has a very low envelope mass ($\lesssim 10^{-2}$ $\mathrm{M}_\odot$)[24,33]. These stars instead evolve directly to the WD cooling track. A HB star can have such a low envelope mass if it suffered extra mass-loss along the previous RGB phase, or if it formed with an elevated helium abundance. In the latter case the higher He affects the evolution of the star such that it arrives on the HB with a lower total mass (for a given GC age). In the former case the mechanisms that might affect the mass loss rates are unknown, although rotation is a possibility[17,34]. In both cases the stars populate the blue end of the HB[7,16,35]. We have calculated some stellar models to compare with the photometric observations. Our models, shown in Figure 3, include standard input physics[36]. The usual Reimers mass-loss rate[37] was used for the RGB and HB. Two model tracks are shown from the MS to the AGB. One has FG composition with the observed He abundance[29] of Y $= 0.245$, the other has SG composition with a moderate He enhancement of δY$= +0.04$. The FG model populates the redder end of the HB, before the Grundahl jump, as expected. It then continues to the AGB. The He-rich SG model (presumed to correspond to the Na-rich population) populates the bluer end of the HB (after the Grundahl jump), and also continues to the AGB. It thus appears that our SG model cannot account for the lack of ascension of the Na-rich BHB stars in this part of the CMD. We note that an increased mass-loss rate during the RGB phase would result in a bluer zero-age HB star, so this can not be a solution since the CMD is clearly populated in this region. One possibility is that the HB stars blueward of the Grundahl jump experience enhanced mass-loss. We show the effect of an ad-hoc 20-fold increase in mass-loss on the SG model during the HB phase (Fig. 3). Indeed this model can populate the blue end of the HB and also fail to become an AGB star. This result again suggests that some physics describing the mass-loss from hot HB stars is missing from the models.

Conclusion

Our conclusive discovery that the majority of stars in NGC 6752 do not enter the AGB phase of evolution has a number of important consequences. For instance, since GCs are often used to test stellar evolution theory, any test which uses star counts of AGB stars will be fundamentally flawed. This is true of the R-Method used to check the lifetimes of various phases of evolution. In particular the R', $R1$ and $R2$ values[11,38,39] all involve the number of AGB stars, so these values will be misleading (including the GC He values inferred from them). This is particularly true if the GCs in question have blue extensions to their HBs, since it is the blue HB stars that appear not to ascend the AGB. Star number counts used to ascertain AGB lifetimes will also be erroneous, unless the proportion of AGB ascenders is known somehow (e.g. via a cut-off in Na abundance or HB colour for AGB ascension). Another consequence is that the results of studies that use integrated light of GCs, usually in the case of unresolved extragalactic GCs, will be affected by the 'loss' of the light contribution from of many of the brightest stars in the clusters. Related to this is the fact that the large population of extreme BHB stars and failed AGB stars will contribute significant UV flux to GCs and extragalactic populations such as elliptical galaxies. Finally, our model results suggest that future stellar models need to include extra physics to model the non-ascension of HB stars. In particular increased mass loss in blue HB stars appears to be needed, most likely blueward of the Grundahl jump.

Methods Summary

Observations of our sample stars (24 RGB + 20 AGB stars, Figure 1 and Table 1) were carried out with the FLAMES-Giraffe spectrograph[40], mounted on the 8.2m telescope at ESO-VLT, under programme 089.D-0038 (PI SWC). We employed the high-resolution grating HR11, which provides a nominal resolution of R $= 24,200$ and a spectral coverage of $\lambda = 5597 \rightarrow 5840$ Å. The LTE Na abundances were obtained from the strong Na I doublet at 5680 Å[41], with the driver $abfind$ in MOOG[42] (2011 version) and the Kurucz set of model atmospheres with no overshooting[43]. Stellar parameters were derived in the following way: T_{eff} values are calculated from a Strömgren colour (b-y) calibration[44]; gravities were then computed from stellar luminosities and the derived temperatures (we assumed a mass of $\mathrm{M} = 0.8\ \mathrm{M}_\odot$ and a distance modulus of $(m-M)V = 13.30$), while microturbulence values ξ were obtained using a relation from the literature[45]. A metallicity of $[\mathrm{Fe/H}] = -1.54$ dex[23] was adopted for all of our sample stars. Although the lines under scrutiny are known to be only marginally affected by departures from LTE, we applied NLTE corrections to our Na abundances[46]. The random (internal) uncertainties (see Table 1) were estimated by adding in quadrature errors due to the EW measurements and those related to stellar parameters. The latter were evaluated in the standard way, that is varying one parameter at a time (keeping the others unchanged) and inspecting the corresponding variation in the resulting abundances. We adopted errors of $\Delta\mathrm{T}_{eff} = \pm 30$ K, $\Delta\,\mathrm{logg} = 0.1$, $\Delta\xi = 0.1$ km/s, and $\Delta[\mathrm{Fe/H}] = \pm 0.05$ dex.

The stellar models presented in Figure 3 were calculated using the Monash University stellar structure code MONSTAR[36, 47, 48]. The code has been recently updated with low temperature opacity tables which follow variations in C, N and O[49].

References

1. Chandrasekhar, S. *An Introduction to the Study of Stellar Structure.* (Dover Publications, New York, 1957).
2. Clayton, D. D. *Principles of Stellar Evolution and Nucleosynthesis* (University of Chicago Press, Chicago, 1983).

3. Kippenhahn, R. & Weigert, A. *Stellar Structure and Evolution* (Springer-Verlag, Berlin, 1990).
4. Bellazzini, M. *et al.* Age as the Second Parameter in NGC 288/NGC 362? I. Turnoff Ages: A Purely Differential Comparison. *AJ* **122**, 2569–2586 (2001).
5. Harbeck, D., Smith, G. H. & Grebel, E. K. CN Abundance Variations on the Main Sequence of 47 Tucanae. *AJ* **125**, 197–207 (2003).
6. Carretta, E., Bragaglia, A., Gratton, R. & Lucatello, S. Na-O anticorrelation and HB. VIII. Proton-capture elements and metallicities in 17 globular clusters from UVES spectra. *A&A* **505**, 139–155 (2009).
7. Iben, I., Jr. & Rood, R. T. Metal-Poor Stars. III. on the Evolution of Horizontal-Branch Stars. *ApJ* **161**, 587 (1970).
8. Renzini, A. & Fusi Pecci, F. Tests of evolutionary sequences using color-magnitude diagrams of globular clusters. *ARA&A* **26**, 199–244 (1988).
9. Landsman, W. B. *et al.* Ultraviolet Imagery of NGC 6752: A Test of Extreme Horizontal Branch Models. *ApJL* **472**, L93 (1996).
10. Grundahl, F., Catelan, M., Landsman, W. B., Stetson, P. B. & Andersen, M. I. Hot Horizontal-Branch Stars: The Ubiquitous Nature of the "Jump" in Strömgren u, Low Gravities, and the Role of Radiative Levitation of Metals. *ApJ* **524**, 242–261 (1999).

11. Sandquist, E. L. & Bolte, M. Exploring the Upper Red Giant and Asymptotic Giant Branches: The Globular Cluster M5. *ApJ* **611**, 323–337 (2004).

12. Campbell, S. W. *et al.* The Case of the Disappearing CN-strong AGB stars in Galactic Globular Clusters - Preliminary Results. *MmSAI* **81**, 1004 (2010).

13. Campbell, S. W. *et al.* Cyanogen in NGC 1851 Red Giant Branch and Asymptotic Giant Branch Stars: Quadrimodal Distributions. *ApJL* **761**, L2 (2012).

14. Norris, J., Cottrell, P. L., Freeman, K. C. & Da Costa, G. S. The abundance spread in the giants of NGC 6752. *ApJ* **244**, 205–220 (1981).

15. Gratton, R. G., Carretta, E. & Bragaglia, A. Multiple populations in globular clusters. Lessons learned from the Milky Way globular clusters. *A&ARv* **20**, 50 (2012).

16. D'Antona, F., Caloi, V., Montalbán, J., Ventura, P. & Gratton, R. Helium variation due to self-pollution among Globular Cluster stars. Consequences on the horizontal branch morphology. *A&A* **395**, 69–75 (2002).

17. Villanova, S., Geisler, D., Piotto, G. & Gratton, R. G. The Helium Content of Globular Clusters: NGC 6121 (M4). *ApJ* **748**, 62 (2012).

18. Smith, G. H. & Norris, J. E. CN variations among asymptotic giant branch and horizontal branch stars in the intermediate metallicity globular clusters M5, M4, and NGC 6752. *AJ* **105**, 173–183 (1993).

19. Yong, D., Grundahl, F., Johnson, J. A. & Asplund, M. Nitrogen Abundances in Giant Stars of the Globular Cluster NGC 6752. *ApJ* **684**, 1159–1169 (2008).

20. Lardo, C. *et al.* C and N abundances of main sequence and subgiant branch stars in NGC 1851. *A&A* **541**, A141 (2012).

21. Smith, G. H. & Tout, C. A. The production of surface carbon depletions among globular cluster giants by interior mixing. *MNRAS* **256**, 449–456 (1992).

22. Angelou, G. C., Stancliffe, R. J., Church, R. P., Lattanzio, J. C. & Smith, G. H. The Role of Thermohaline Mixing in Intermediate- and Low-metallicity Globular Clusters. *ApJ* **749**, 128 (2012).

23. Carretta, E., Bragaglia, A., Gratton, R. G., Lucatello, S. & Momany, Y. Na-O anticorrelation and horizontal branches. II. The Na-O anticorrelation in the globular cluster NGC 6752. *A&A* **464**, 927–937 (2007).

24. D'Cruz, N. L., Dorman, B., Rood, R. T. & O'Connell, R. W. The Origin of Extreme Horizontal Branch Stars. *ApJ* **466**, 359 (1996).

25. Cassisi, S., Salaris, M. & Irwin, A. W. The Initial Helium Content of Galactic Globular Cluster Stars from the R-Parameter: Comparison with the Cosmic Microwave Background Constraint. *ApJ* **588**, 862–870 (2003).

26. Cassisi, S., Castellani, V., Degl'Innocenti, S., Piotto, G. & Salaris, M. Asymptotic Giant Branch predictions: Theoretical uncertainties. *A&A* **366**, 578–584 (2001).

27. Marino, A. F. *et al.* Sodium-Oxygen Anticorrelation Among Horizontal Branch Stars in the Globular Cluster M4. *ApJL* **730**, L16 (2011).

28. Briley, M. M. CN and CH band strengths of 283 47 tucanae giants. *AJ* **114**, 1051–1059 (1997).

29. Villanova, S., Piotto, G. & Gratton, R. G. The helium content of globular clusters: light element abundance correlations and HB morphology. I. NGC 6752. *A&A* **499**, 755–763 (2009).

30. Momany, Y. *et al.* A New Feature along the Extended Blue Horizontal Branch of NGC 6752. *ApJL* **576**, L65–L68 (2002).

31. Hubrig, S. *et al.* A high-resolution study of isotopic composition and chemical abundances of blue horizontal branch stars in the globular clusters NGC 6397 and NGC 6752. *A&A* **499**, 865–878 (2009).

32. Greggio, L. & Renzini, A. Clues on the hot star content and the ultraviolet output of elliptical galaxies. *ApJ* **364**, 35–64 (1990).

33. Caloi, V. Evolution of extreme horizontal branch stars. *A&A* **221**, 27–35 (1989).

34. Gratton, R. G. *et al.* The Na-O anticorrelation in horizontal branch stars. III. 47 Tucanae and M 5. *A&A* **549**, A41 (2013).

35. Sweigart, A. V. & Gross, P. G. Horizontal-Branch Evolution with Semiconvection II. Theoretical Sequences. *ApJS* **32**, 367 (1976).

36. Campbell, S. W. & Lattanzio, J. C. Evolution and nucleosynthesis of extremely metal-poor and metal-free low- and intermediate-mass stars. I. Stellar yield tables and the CEMPs. *A&A* **490**, 769–776 (2008).

37. Reimers, D. Circumstellar absorption lines and mass loss from red giants. *Memoires of the Societe Royale des Sciences de Liege* **8**, 369–382 (1975).

38. Iben, I. & Rood, R. T. Ratio of Horizontal Branch Stars to Red Giant Stars in Globular Clusters. *Nature* **224**, 1006–1008 (1969).

39. Buonanno, R., Corsi, C. E. & Fusi Pecci, F. The giant, asymptotic, and horizontal branches of globular clusters. II - Photographic photometry of the metal-poor clusters M15, M92, and NGC 5466. *A&A* **145**, 97–117 (1985).

40. Pasquini, L. *et al.* Installation and commissioning of FLAMES, the VLT Multifibre Facility. *The Messenger* **110**, 1–9 (2002).

41. Gratton, R. G., Carretta, E., Claudi, R., Lucatello, S. & Barbieri, M. Abundances for metal-poor stars with accurate parallaxes. I. Basic data. *A&A* **404**, 187–210 (2003).

42. Sneden, C. A. *Carbon and Nitrogen Abundances in Metal-Poor Stars.* Ph.D. thesis, The University of Texas at Austin. (1973).

43. Kurucz, R. ATLAS9 Stellar Atmosphere Programs and 2 km/s grid. *CD-ROM No. 13., Smithsonian Astrophysical Observatory, Cambridge, Mass.* **13** (1993).

44. Alonso, A., Arribas, S. & Martínez-Roger, C. Erratum: The effective temperature scale of giant stars (F0-K5). II. Empirical calibration of T$_{eff}$ versus colours and [Fe/H]. *A&A* **376**, 1039 (2001).

45. Gratton, R. G., Carretta, E. & Castelli, F. Abundances of light elements in metal-poor stars. I. Atmospheric parameters and a new T$_{eff}$ scale. *A&A* **314**, 191–203 (1996).

46. Gratton, R. G., Carretta, E., Eriksson, K. & Gustafsson, B. Abundances of light elements in metal-poor stars. II. Non-LTE abundance corrections. *A&A* **350**, 955–969 (1999).

47. Wood, P. R. & Zarro, D. M. Helium-shell flashing in low-mass stars and period changes in mira variables. *ApJ* **247**, 247–256 (1981).

48. Lattanzio, J. C. The asymptotic giant branch evolution of 1.0-3.0 solar mass stars as a function of mass and composition. *ApJ* **311**, 708–730 (1986).

49. Marigo, P. & Aringer, B. Low-temperature gas opacity. ÆSOPUS: a versatile and quick computational tool. *A&A* **508**, 1539–1569 (2009).

50. Clem, J. L., VandenBerg, D. A., Grundahl, F. & Bell, R. A. Empirically Constrained Color-Temperature Relations. II. uvby. *AJ* **127**, 1227–1256 (2004).

Acknowledgements We thank Dr. Yazan Momany of ESO (Chile) for providing his UBV photometric dataset which is mentioned in the paper. S.W.C. acknowledges support from the Australian Research Council's Discovery Projects funding scheme (project DP1095368). F.G. acknowledges funding for the

Stellar Astrophysics Centre provided by The Danish National Research Foundation. The research is supported by the ASTERISK project funded by the European Research Council (Grant agreement no.: 267864). This work was based on observations made with ESO telescopes at the La Silla Paranal Observatory under programme ID 089.D-0038 and made extensive use of the SIMBAD, Vizier, 2MASS, and NASA ADS databases.

Author Contributions S.W.C. designed and prepared the ESO/VLT observing proposal, collected the spectroscopic data, and prepared the paper. V.D. reduced and analysed the spectroscopic data, and prepared the paper. D.Y. designed and prepared the ESO/VLT observing proposal and assisted in the paper preparation. T.N.C. calculated the stellar models and prepared figures for the paper. J.C.L. assisted in the preparation of the observing proposal and with the paper preparation. R.J.S., G.C.A. and E.C.W. assisted in the paper preparation and made the preliminary cyanogen observations with the Anglo-Australian Telescope mentioned in the paper. F.G. provided the $uvby$ photometric data for the AGB and RGB sample and assisted in the paper preparation.

Author Information Reprints and permissions information is available at www.nature.com/reprints. Correspondence and requests for materials should be addressed to simon.campbell@monash.edu.

Table 1: **The stellar sample including atmospheric parameters and Na abundances.**

Type	ID	T$_{eff}$	$\log$ (g)	ξ	$\log$ (N$_{Na}$)	[Na/Fe]	Error
AGB	FGJ000022	4607	1.414	1.765	4.85	0.06	0.09
AGB	FGJ000025	4371	1.146	1.851	4.71	-0.08	0.09
AGB	FGJ000031	4460	1.285	1.806	4.73	-0.06	0.09
AGB	FGJ000044	4629	1.537	1.725	4.63	-0.16	0.07
AGB	FGJ000052	4787	1.740	1.660	4.74	-0.05	0.09
AGB	FGJ000053	4688	1.636	1.693	4.73	-0.06	0.10
AGB	FGJ000059	4772	1.719	1.666	4.82	0.03	0.06
AGB	FGJ000060	4685	1.654	1.687	4.58	-0.21	0.10
AGB	FGJ000061	4714	1.689	1.676	4.69	-0.10	0.10
AGB	FGJ000065	4677	1.540	1.724	4.91	0.12	0.14
AGB	FGJ000075	4763	1.764	1.652	4.55	-0.24	0.07
AGB	FGJ000076	4881	1.850	1.624	4.74	-0.05	0.05
AGB	FGJ000078	4868	1.855	1.623	4.82	0.03	0.07
AGB	FGJ000080	4829	1.843	1.627	4.67	-0.12	0.08
AGB	FGJ000083	4825	1.849	1.625	4.66	-0.13	0.08
AGB	FGJ000089	4861	1.868	1.618	4.80	0.01	0.04
AGB	FGJ000094	4925	1.937	1.596	4.75	-0.04	0.10
AGB	FGJ000097	4946	1.978	1.583	4.74	-0.05	0.05
AGB	FGJ000104	4874	1.907	1.606	4.56	-0.23	0.08
AGB	FGJ201620	4864	1.938	1.596	4.74	-0.05	0.11
RGB	FGJ000012	4270	1.062	1.878	5.06	0.27	0.12
RGB	FGJ000023	4360	1.181	1.840	5.18	0.39	0.12
RGB	FGJ000027	4425	1.290	1.805	4.75	-0.04	0.11
RGB	FGJ000029	4298	1.102	1.865	4.67	-0.12	0.12
RGB	FGJ000030	4294	1.070	1.876	5.13	0.34	0.10
RGB	FGJ000035	4439	1.353	1.784	5.41	0.62	0.10
RGB	FGJ000043	4443	1.359	1.782	5.49	0.70	0.10
RGB	FGJ000050	4404	1.267	1.812	5.02	0.23	0.13
RGB	FGJ000054	4496	1.487	1.741	4.92	0.13	0.12
RGB	FGJ000064	4436	1.353	1.784	5.42	0.63	0.12
RGB	FGJ000069	4583	1.587	1.709	5.34	0.55	0.12
RGB	FGJ000091	4665	1.776	1.648	5.12	0.33	0.11
RGB	FGJ000092	4612	1.711	1.669	4.73	-0.06	0.10
RGB	FGJ000107	4662	1.822	1.633	5.01	0.22	0.11
RGB	FGJ000129	4717	1.939	1.596	5.03	0.24	0.09
RGB	FGJ000155	4726	1.992	1.579	4.62	-0.17	0.07
RGB	FGJ000161	4775	2.052	1.559	5.17	0.38	0.05
RGB	FGJ000170	4794	2.083	1.549	5.33	0.54	0.12
RGB	FGJ000186	4800	2.117	1.538	4.70	-0.09	0.10
RGB	FGJ000193	4806	2.134	1.533	4.55	-0.24	0.04
RGB	FGJ000217	4813	2.161	1.524	5.22	0.43	0.05
RGB	FGJ000262	4855	2.252	1.495	5.13	0.34	0.09
RGB	FGJ000276	4858	2.260	1.492	5.15	0.36	0.11
RGB	FGJ200619	4760	1.940	1.595	5.43	0.64	0.11

The evolutionary status of each star is indicated in column 1. ID codes are designations of the current study. T$_{eff}$, $\log$ (g), and ξ are the surface temperature, gravity, and microturbulence values used in the abundance determinations. $\log$ (N$_{Na}$) and [Na/Fe] are the final Na abundances. The final column shows the internal errors in [Na/Fe].

Figure 1 Sample selection in the Strömgren $uvby$ colour-magnitude diagram of NGC 6752. Small black dots show the whole photometric sample[10]. Our AGB and RGB stellar samples are shown as blue squares and red triangles respectively. Part of the horizontal branch can be seen at bottom left, at y magnitudes $\gtrsim 13.5$.

Figure 2 Sodium abundance results for NGC 6752. Results for our sample of RGB stars (filled red triangles, 24 stars) and AGB stars (filled blue squares, 20 stars) are shown. Error bars show internal abundance determination uncertainties. For comparison the RGB results of a previous study (C07)[23] are included (grey open circles). The horizontal dotted line at [Na/Fe] $= 0.18$ delineates the upper envelope of AGB values, and serves as the definition between Na-rich and Na-poor stars.

Figure 3 Theoretical stellar model tracks overlain on the Strömgren colour-magnitude diagram of NGC 6752. The solid red line (with open circle symbols marking 5 million year time intervals) is a model with an initial mass of 0.80 $M_\odot$ and a helium content of Y $= 0.245$. This Y value matches that reported for the redder end of the HB[29]. This FG model does indeed spend most of its HB evolution at the red end of the HB. The solid black line (with open square symbols marking 5 million year time intervals) is a model with an initial mass of 0.75 $M_\odot$ and a helium content of Y $= 0.285$. This SG model spends its HB evolution in a bluer part of the HB, but still ascends the AGB, contrary to what is inferred from the observations in the current study. The solid blue line (with open triangle symbols marking 5 million year time intervals) shows the evolution of the $Y = 0.285$ model with an ad-hoc

20-fold increase in mass-loss rate ($\dot{M} = dM/dt$) initiated once the star settles on the HB. This model evolves downwards along the extreme blue end of the HB and fails to ascend the AGB. The arrow indicates the location of the Grundahl jump at $y = 14.65$ (see text for details). Transforms from theoretical luminosity-T$_{eff}$ plane to CMD have been made[50].

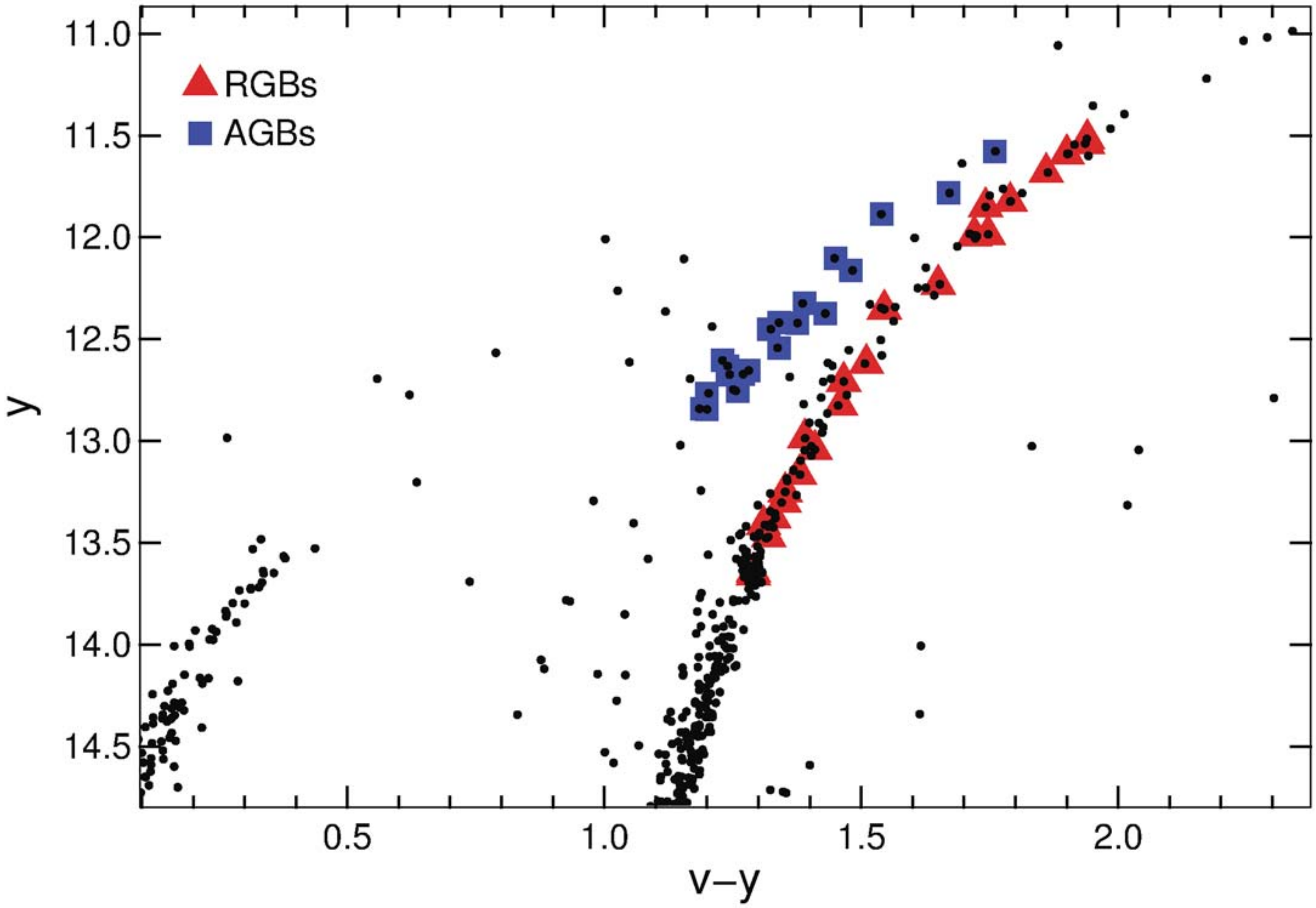
RGBs
AGBs
y
11.0
11.5
12.0
12.5
13.0
13.5
14.0
14.5
0.5
1.0
1.5
2.0
v−y

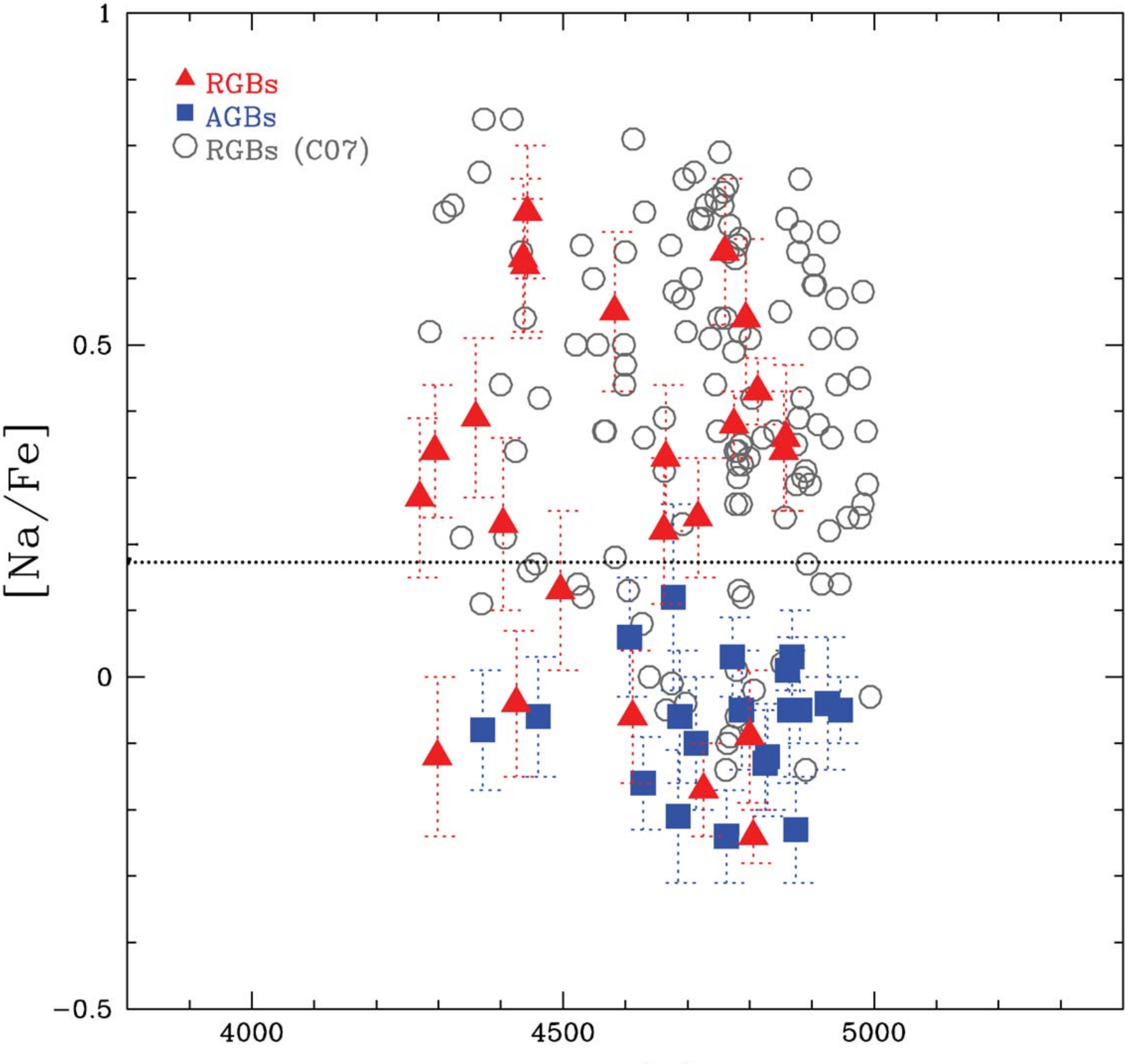

RGBs
AGBs
RGBs (C07)
1
0.5
0
−0.5
4000
4500
5000
[Na/Fe]
T_{eff} (K)

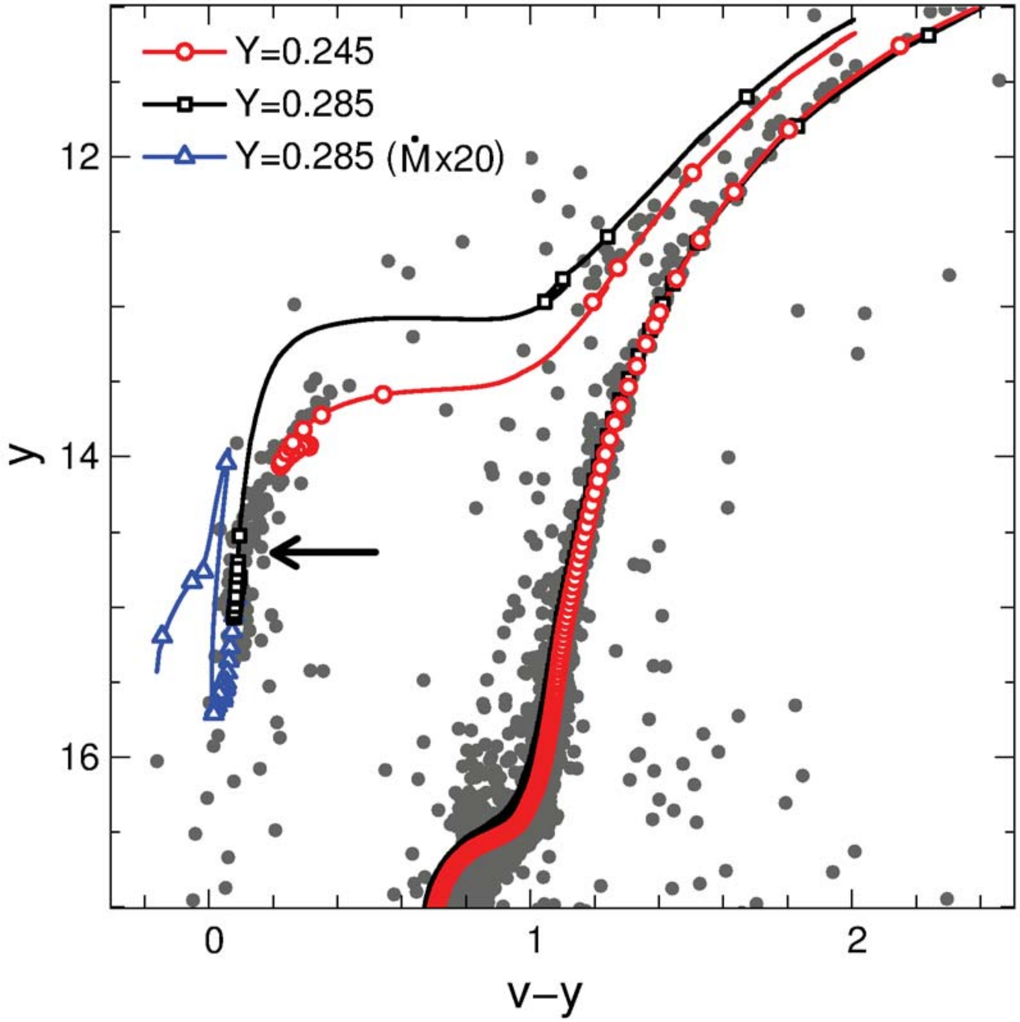
Y=0.245
Y=0.285
Y=0.285 ($\dot{M}$x20)
12
14
16
y
0
1
2
v−y